

# Transient Response of Hybrid Boolean Networks as Physical Unclonable Functions

Daniel Canaday<sup>1,2</sup>, Noeloikeau Charlot<sup>1</sup>, Andrew Pomerance<sup>2</sup> and Daniel J. Gauthier<sup>1</sup>

<sup>1</sup> Ohio State University, Department of Physics, 191 West Woodruff Ave, Columbus, OH 43202, USA [canaday.14@osu.edu](mailto:canaday.14@osu.edu)

<sup>2</sup> Potomac Research, LLC, 2597 Nicky Lane Alexandria, VA 22311, USA

**Abstract.** Physical unclonable functions are devices that exploit small, random variations in a manufacturing process to create unique and stable identifying behavior. These devices have found a variety of security applications, from intellectual property protection to secret key generation. In this work, we propose a framework for constructing physical unclonable functions from hybrid Boolean networks realized on field-programmable gate arrays. These networks are highly sensitive to propagation delay and other non-ideal behavior introduced by the silicon fabrication process and thus provide a source of entropy generation that is amplified by chaotic dynamics. We leverage this behavior in the context of physical unclonable functions by setting the initial state of the network to a specified Boolean string (the challenge) and measuring the state of the network some time later (the response). Due to the non-equilibrium nature of the proposed protocol, challenge-response pairs can be collected at a rapid rate of up to 100 MHz. Moreover, we collect multiple response bits per challenge, in contrast to many proposed techniques. We find a high degree of reliability and uniqueness from the proposed devices, respectively characterized by  $\mu_{intra} = 6.68\%$  and  $\mu_{inter} = 47.25\%$  for a moderately sized device. We estimate the available entropy in devices of varying size with several statistical tests and find that the entropy scales exponentially with the size of the network.

**Keywords:** Physical Unclonable Functions · Field Programmable Gate Arrays · Boolean networks

## 1 Introduction

The creation, storage, and distribution of cryptographic keys remains an active area of research due to the ever-increasing demand for privacy protection and secure computing [ZDMW16, BH15, TŠK07]. One attractive approach towards these problems is the concept of a physical unclonable function (PUF). A PUF with the appropriate security properties is capable of generating secure keys “on the fly,” and effectively storing them in the physical details of the device. Some devices, so-called “strong PUFs” [RBK10, MBW<sup>+</sup>19], contain an exponentially large number of independent keys, making attempts to extract all of them from a compromised device a difficult or impossible task.

Physical unclonable functions are physical devices that process an input, called a *challenge*, and produce an output, called a *response*. A particular PUF instance is a member of a PUF class, all the members of which are created by some construction process that is subject to small, random variations. To be appropriate for security applications, PUFs must have the following properties:

- *Reliability:* Given a particular PUF instance, the responses resulting from successive evaluations of the same challenge are identical up to a small error.

- *Uniqueness*: Given two PUF instances and a particular challenge, the resulting responses are very different.
- *Unclonability*: Due to the nature of the construction process, no two PUF instances are likely to have identical challenge-response behavior.
- *Unpredictability*: Even with knowledge of the construction process, it is difficult or impossible to infer the response to one challenge given the response to a different challenge.

In this work, we propose a strong PUF class that has these properties, which we quantify in Sections 4 and 5. A response to a given challenge can be extracted from a PUF instance in as little as 10 ns. The PUFs require only a small number of resources for a desired amount of entropy in comparison to similar PUF proposals fabricated in silicon. Further, the presence of chaos in the challenge-response process may result in resilience to machine-learning based attacks [LHH18].

The proposed device is a hybrid of an autonomous Boolean network (ABN) and synchronous, clocked logic, resulting in a hybrid Boolean network (HBN). It is constructed on a readily-available electronic platform known as a field-programmable gate array (FPGA). The autonomous portion of the network is based on a variant of a physical random number generator known to produce random bits at a rate of 100 Mb/s [Ros15, RRG13]. The evolution of the HBN from an initial state is highly sensitive to the manufacturing details, including propagation delays and degradation effects. We leverage this phenomenon to construct a class of PUFs by considering the challenge to be the initial state of the ABN and the response to be the state of the synchronous portion some time later.

The rest of this paper is outlined as follows. In Section 2, we describe our proposed HBN-PUF design in detail. In Section 3, we describe the setup of the experiments used to validate the proposed design. In Section 4, we discuss the reliability and uniqueness measurements. In Section 5, we discuss a number of entropy estimates. Finally, we conclude and discuss further research directions in Section 6.

## 2 HBN-PUF Design

In this section, we describe the details of the HBN-PUF and its implementation, including how responses are produced from challenges. As motivation, we begin by describing previous work on a similarly designed HBN for random number generation.

### 2.1 HBN for Random Number Generation

As noted in the introduction, much attention in the field of cryptography is devoted towards cryptographic keys. Many protocols for secure communication, including the popular Rivest–Shamir–Adleman cryptosystem [JK03], rely on the generation of random numbers for encryption of secure data. Generating random numbers as quickly as possible prevents the storage of encryption keys and thereby increases the security of their usage.

One approach to random number generation that produces extremely high random bit rates is based on an HBN [Ros15, RRG13] and referred to here as an HBN-RNG. The idea is to create a chaotic physical system on an FPGA whose dynamics rapidly approach the maximum frequency allowed by the hardware due to the finite rise- and fall-times of the logic elements (LEs) on the FPGA. The system should also exhibit self-excitation and not be biased towards logical high or low.

A circuit satisfying these properties can be realized with a particular HBN and is depicted in Figure 1a-1d. The ABN is formed from a ring of  $N$  nodes, where each node is bidirectionally coupled along the ring as well as coupled to itself. All but one of the nodes

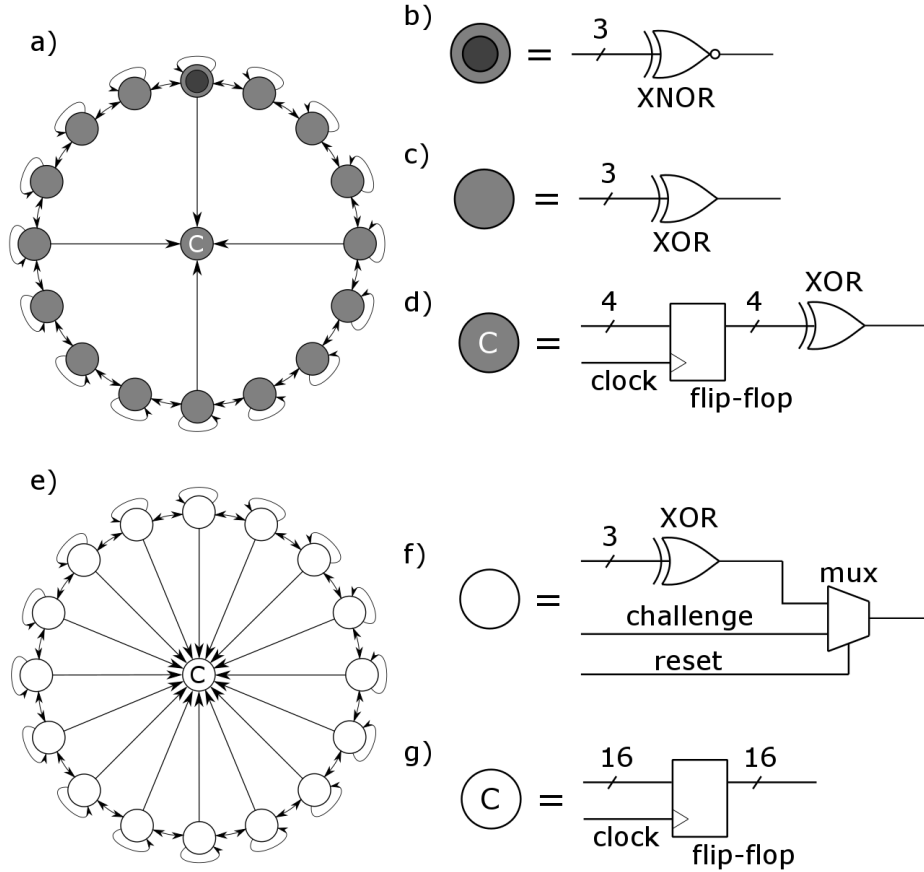


**Figure 1:** a) A size  $N = 16$  HBN-RNG. Random numbers are read from the state of the clocked readout. b-d) The components of the HBN-RNG, where the number appearing above wires indicates how many wires are present. e) A  $N = 16$  HBN-PUF. The response is read from the clocked readout after one clock cycle. The initial conditions of the autonomous portion are specified by the challenge string. The network is released from initial conditions by changing the value of the RESET bit. The response is read only a short time after release from initial conditions, and is therefore highly dependent upon the challenge and small differences in propagation delays and degradation effects within the nodes. f, g) The components of the HBN-PUF. Again, the number appearing above wires indicates how many wires are present.

execute the 3-input XOR operation, returning 1 if an even number of inputs are 1, and 0 otherwise. One of the nodes instead executes the XNOR operation, which is the logical negation of the XOR operation. This node breaks the rotational symmetry of the ring and forces self-excitation of the system.

The clocked portion of the HBN-RNG is a clocked-readout that registers the state of 4 of the ABN nodes on the rising edge of some global clock. To ensure an unbiased output, the registered values are passed through a final XOR gate to reduce the bias in the output bit stream.

A transition to chaos in the HBN-RNG occurs at  $N = 5$  above which the network becomes exponentially sensitive to initial conditions and LE parameter details. An efficient RNG can be realized with 128 copies of  $N = 16$  networks running in parallel, resulting in a 12.8 GHz random bit rate.

## 2.2 HBN Physical Unclonable Functions

The physical random number generator described above is "PUF-like" in a number of ways. First, the dynamics are highly sensitive to initial conditions and details of their underlying physical circuitry. These properties follow from the presence of chaos and together imply the uniqueness property discussed in Section 1. Second, the HBN-RNG and similar ABNs [DLHG16] have transients that can last many orders-of-magnitude longer than the characteristic time-scale of the network, which is on the order of hundreds of picoseconds. This suggests a window of stability in the transient HBN response, where the network state is reliable in the sense discussed in Section 1 while retaining significant information about the physical details.

With these considerations in mind, the HBN-RNG scheme can be modified to act as a physical unclonable function or HBN-PUF. In particular, we make the following changes:

- Replace each node with an XOR LE and a multiplexer that sets the initial state of the ABN to a particular value, as shown in Figure 1f.
- Read the *entire ABN state* at the clocked readout, once, on a timescale comparable to the correlation time of the ABN, thereby capturing the transient response of the network. This is shown in Figure 1g.

The first change is to make the network challengeable, as will be discussed later in this section. Note that the XNOR node is also replaced with an XOR node so that the ring is symmetric and does not self-excite from the all-0 state.

The second change is to ensure that the state of the clocked readout is correlated with the initial state, containing information about it in some complicated way. The idea here is that the transient response of the network depends both on the initial conditions *and* the details of the LEs that form the HBN. Because the transient is short-lasting, we only make one measurement of the clocked readout to form the response.

The proposed HBN-PUF is challenged by a binary string  $C$  by setting the initial state of the network to  $C$ , according to some fixed but arbitrary labeling of the nodes. At  $t = 0$ , the RESET bit is flipped to 0, allowing the ABN to evolve. At a short time  $\tau$  later, the state of the ABN is registered by the clocked readout and is later read by an on-chip memory controller. The measured state of the clocked readout is the response  $R$  of the HBN-PUF to the challenge  $C$ . A schematic of the HBN-PUF is shown in Figure 1e.

It is clear from the description above that an HBN-PUF class is characterized by two parameters  $N$  and  $\tau$ . Each device of size  $N$  requires  $3N$  FPGA resources to synthesize (the extra element per node being the multiplexer, compared to the HBN-RNG). We refer to  $\tau$  as the measurement time.

### 3 Experimental Setup

To characterize and validate our proposed design, we synthesize the HBNs on a Cyclone V GX 5CGXFC5C6F27C7N FPGA. To efficiently characterize intra-device statistics, we synthesize many different oscillators at different locations on a single chip and challenge them simultaneously. The physical differences in the LEs that form the different oscillators are proxies for the physical differences in oscillators fabricated on separate chips.

The HBN-PUFs are characterized by  $N$  and  $\tau$ , as discussed in Section 2.2. In principle,  $\tau$  should be optimized in a way that depends on the LE timescales and potentially  $N$ . However, we find that  $\tau$  is best kept as small as the FPGA’s global clock allows, or about 5 ns for the FPGA used in these experiments. We therefore fix  $\tau = 5$  ns, but note that the effective measurement time might potentially be reduced by various means.

Experiments on a PUF class are further characterized by the number of synthesized oscillators  $N_{osc}$ , the number of challenges  $N_{chal}$  for which responses from each oscillator are measured, and the number of measurements  $N_{meas}$  for each PUF and challenge. As noted in Section 2.2, a single PUF of size  $N$  requires only  $3N$  LEs to synthesize, including reset logic and synchronous measurement logic. This means that extremely large PUFs are possible on modern FPGAs, which can feature one million or more LEs. However, we focus on smaller  $N$  to acquire good statistics on various performance metrics in the following sections.

We consider the space of valid challenges to be all possible bit strings of length  $N$  that are not steady-states. For all  $N$ , this means we exclude the all-0 or all-1 state. For even  $N$ , we must also exclude the states with alternating 0’s and 1’s. Thus, the number of valid challenges is given by

$$N_{vc} = \begin{cases} 2^N - 2 & N \text{ odd} \\ 2^N - 4 & N \text{ even.} \end{cases} \quad (1)$$

In either case, the number of bits read per challenge is  $N$ . The extractable bits from our proposed design may potentially scale as  $N2^N$ , resulting in a strong PUF.

## 4 Reliability and Uniqueness

In this section, we discuss reliability and uniqueness tests based on measurements of intra- and inter-device statistics. We first define some notation and explain how the statistics quantify that reliability and uniqueness properties discussed in Section 1. We then describe the experiments and discuss their results.

### 4.1 Intra- and Inter-Device Statistics

Let  $\mathcal{P}$  be the set of all possible PUFs belonging to a certain PUF class, and let  $\mathcal{C}$  be the set of all valid challenges for that class. A response of a PUF instance  $P$  in  $\mathcal{P}$  on a challenge  $C$  in  $\mathcal{C}$  is a measurement of a random variable  $R$  whose distribution depends on  $P$  and  $C$ , *i.e.*,

$$R_P(C) \leftarrow P(C). \quad (2)$$

Broadly speaking, we want to quantify the reliability and uniqueness of the PUF class by studying the distribution of various functions of  $R$ . In particular, reliability is related to  $R$  when different measurements correspond to the *same* PUF and *same* challenge. On the other hand, uniqueness is related to  $R$  when different measurements correspond to *different* PUFs and the *same* challenge.

Towards the ends mentioned above, we define the following random variable

$$D_P^{intra}(C) = \text{dist}(R_P(C), R'_P(C)), \quad (3)$$

where  $\text{dist}(R_P(C), R'_P(C))$  is the fractional Hamming distance between two distinct response measurements  $R_P(C)$  and  $R'_P(C)$  on a *fixed* PUF instance  $P$  on a given challenge  $C$ . The fractional Hamming distance is defined as the proportion of differing bits between two binary strings. Similarly, we define

$$D_{P,P'}^{inter}(C) = \text{dist}(R_P(C), R_{P'}(C)), \quad (4)$$

where  $\text{dist}(R_P(C), R_{P'}(C))$  is the fractional Hamming distance between two distinct response measurements  $R_P(C)$  and  $R_{P'}(C)$  on two *different* PUF instances  $P$  and  $P'$  on a given challenge  $C$ .

The statistics of the first random variable  $D_P^{intra}(C)$  quantify the reliability of the response of a given PUF to a given challenge because it corresponds to the difference in successive responses of a single PUF to a single challenge. Ideally, the PUF produces a response free of error, in which case  $D_P^{intra}(C)$  is 0 with probability 1 for each PUF  $P$  and challenge  $C$ . On the other hand,  $D_{P,P'}^{inter}(C)$  is a measure of uniqueness, or the ability to distinguish two PUF instances  $P$  and  $P'$ , because it corresponds to difference in responses of two different PUF instances. If the PUF instances are perfectly distinguishable, then the response of PUF  $P$  will have no correlation with the response of PUF  $P'$ , in which case  $D_{P,P'}^{inter}(C)$  will be 0.5 with probability 1 for every pair of PUF instances  $P$  and  $P'$  and challenge  $C$ .

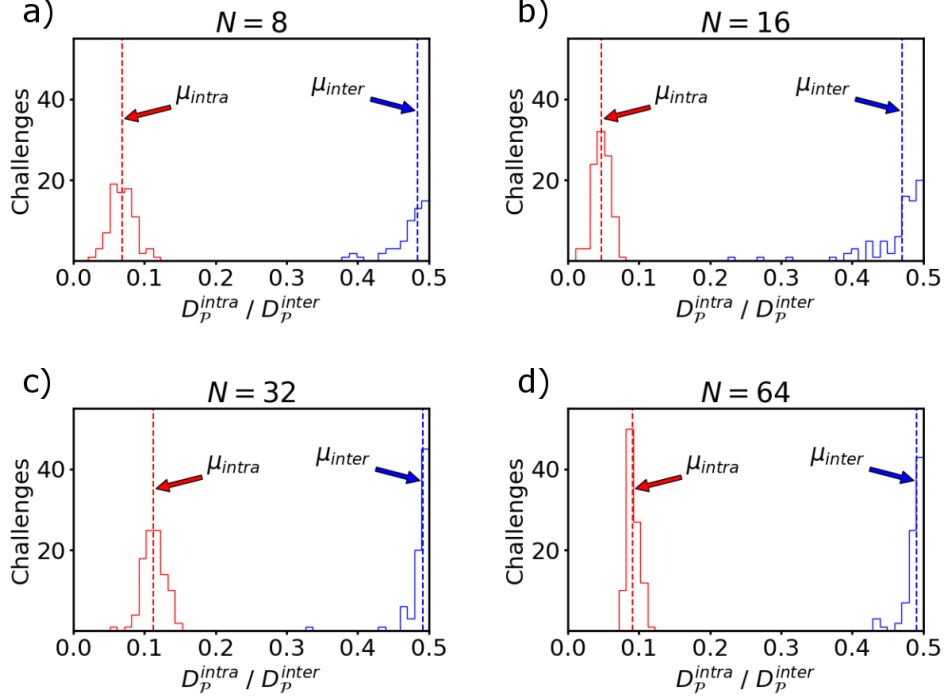


**Figure 2:** Histogram data for intra-device (red) and inter-device (blue) statistics. The means of the distributions are indicated by vertical dashed lines.

## 4.2 Experiments and Results

To understand these distributions, we synthesize  $N_{oscs} = 16$  for various values of  $N$ . The response of each of these oscillators to  $N_{chal} = 100$ , chosen randomly, is repeatedly measured  $N_{meas} = 20$  times. We average the data over PUF instances and plot the distributions in Figure 2, which approximate  $D_{\mathcal{P}}^{intra/inter}(C)$ . The means of these distributions are commonly referred to as  $\mu_{intra}$  and  $\mu_{inter}$ , respectively, and are represented by vertical dashed lines. These values indicate the reliability and uniqueness of two randomly chosen PUF instances with respect to a randomly chosen challenge.

We find the  $\mu_{inter}$  to be close to the ideal value of 0.5 for the values of  $N$  investigated. We find that  $\mu_{intra}$  increases slightly from 0.05 to 0.1, away from the ideal value of 0. Further, it is clear from Figure 2 that the tightness of these distributions increases with increasing  $N$ . The large separation of the distributions indicates that PUF instances are highly distinguishable from a small number of challenge-response pairs. They further confirm the motivation for the HBN-PUF as discussed in Section 3, *i.e.*, that the transient response of the HBN is highly correlated with the initial state (hence the small value of  $\mu_{intra}$ ) and is very sensitive to small differences in the LEs that form the HBN (hence  $\mu_{inter}$  being close to 0.5).

## 5 Entropy Analysis

In the security analysis of PUFs, the extractable entropy is of central importance. This quantity is ultimately related to both reliability and uniqueness and provides an upper-bound on the amount of information that can be securely exchanged with a PUF instance [TSS<sup>+</sup>05]. The extractable entropy is difficult to estimate directly, as it is formed from probability distributions in exponentially high dimensional spaces. We describe in this section several ways to estimate the entropy from limited data. In what follows, all logarithms are in base 2.

### 5.1 Min-Entropy

The min-entropy of a random variable  $X$  is defined as

$$H_{min}(X) = -\log(p_{max}(X)), \quad (5)$$

where  $p_{max}(X)$  is the probability of the most likely outcome. If  $X = (x_1, x_2, \dots, x_n)$  is a vector of  $n$  independent random variables, then the min entropy is

$$H_{min}(X) = \sum_{i=1}^n -\log(p_{max}(x_i)). \quad (6)$$

The entropy is often estimated from Equation 6 in the case of memory-based PUFs [HBF09, SvdSvdL12], where each  $x_i$  is the random variable corresponding to the probability that the  $i$ -th memory cell will be 1 when measured. The independence of these cells is often assumed, although dependencies have been found to exist [Mae16]. Given the explicit coupling in our PUF design, the independence is even less obvious. Nonetheless, we start in this section by assuming independence and calculating the min-entropy. The calculation of the min-entropy scales sub-exponentially with  $N$  and thus allows us to efficiently estimate an upper bound for the entropy of large- $N$  devices. In the next section, we refine this assumption with the empirical mutual information between bit pairs to get a more accurate estimate of the entropy in low  $N$  devices.

In the case of a strong PUF with multiple challenges and a large response space, we need an ordering of the response bits in order to make sense of entropy calculations, such

**Table 1:** An illustration of response-bit ordering for  $N = 3$ , where there are  $3 * 6 = 18$  total bits.

Challenge	Node 1	Node 2	Node 3
001	$x_1$	$x_2$	$x_3$
010	$x_4$	$x_5$	$x_6$
011	$x_7$	$x_8$	$x_9$
100	$x_{10}$	$x_{11}$	$x_{12}$
101	$x_{13}$	$x_{14}$	$x_{15}$
110	$x_{16}$	$x_{17}$	$x_{18}$

**Table 2:** Min entropy and min entropy densities.

$N$	$H_{min}$	$\rho_{min}$
8	$1.6 \times 10^3$	0.80
16	$1.2 \times 10^7$	0.69
32	$3.3 \times 10^{12}$	0.75
64	$5.6 \times 10^{22}$	0.75

as in Equation 6. A natural ordering is to define the response of the  $i$ -th node to the  $j$ -th challenge as  $x_{jN+i}$ , where the challenges are ordered lexicographically. This is illustrated in Table 1 for the simple case of  $N = 3$ . Here, there are only 6 challenges because we omit the trivial all-0 and all-1 challenges, as discussed in Section 3.

Assuming independence of the  $x_i$ , the min-entropy for the HBN-PUF can be readily calculated with Equation 6 from empirical estimates of  $p_{max}(x_i)$ . We estimate these values for  $N = 8, 16, 32, 64$  with  $N_{oscs} = 16$ ,  $N_{chal} = 100$ , and  $N_{meas} = 100$ , as described in Section 3. For each  $x_i$ , the estimate of  $p_{max}(x_i)$  is simply the observed frequency of 0 or 1, whichever is larger. Although we are not measuring these values for all of the possible valid challenges, we assume that the randomly chosen challenges form a representative sample. The results are presented in Table 2.

To put the entropy calculations into context, we also present them as a fraction of the optimal case. If all of the  $x_i$  were independent and completely unbiased, *i.e.*, each  $x_i$  were equally likely to be 0 or 1, than the min-entropy would be equal to  $N$  times the number of valid challenges  $N_{vc}$ . We therefore define the min-entropy density as

$$\rho_{min} = H_{min}/(NN_{vc}), \quad (7)$$

where  $N_{vc}$  is defined in Equation 1.

We see from Table 2 that the HBN-PUFs have min-entropy approximately 70% to 80% of full min-entropy. For comparison, various standard electronic PUFs have min-entropy between 51% and 99%—see, *e.g.*, Reference [Mae16] for a more complete comparison. The HBN-PUF therefore has min-entropy density comparable to state-of-the-art techniques.

Another interpretation of the min-entropy is that it is equal to the number of bits one can securely exchange if an adversary only knew about the biases of the  $x_i$ . From Table 2, one can exchange  $5.6 \times 10^{22}$  bits of information against a naïve adversary. This HBN-PUF uses only  $3 * 64 = 192$  LEs, which is extremely compact compared to other FPGA-based PUF designs, and hence we can easily increase the entropy by increasing the size of the ring.

## 5.2 Impact of Joint Probability Distribution

Although we assume in the previous section that  $x_i$  are independent, this is only approximately the case. Correlations between bit pairs do exist, and some structure to these

correlations appears to develop at higher  $N$ . We study these correlations by calculating the mutual information, defined as

$$I(x_i, x_j) = \sum_{x_i, x_j} p(x_i, x_j) \log \left[ \frac{p(x_i, x_j)}{p(x_i)p(x_j)} \right] \quad (8)$$

between all pairs of  $x_i, x_j$ . Unlike min-entropy, the mutual information is difficult to calculate for higher  $N$ , so we will restrict our attention to  $N = 3 - 8$ . We calculate the mutual information for small  $N$  with  $N_{oscs} = 32$ ,  $N_{chal} = N_{vc}$ , and  $N_{meas} = 100$ . For  $N = 7$ , regions with non-trivial mutual information ( $> 0.05$  bits) are shown in Figure 3.

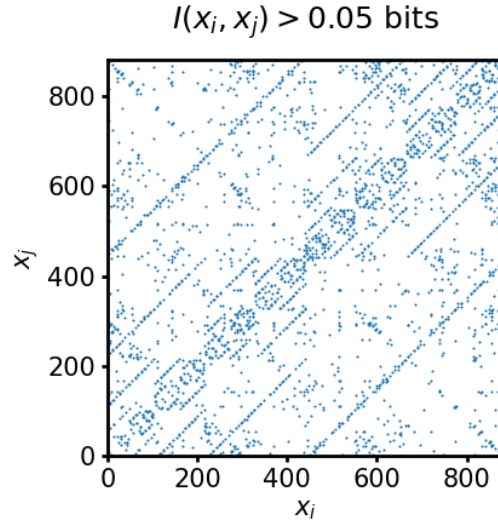


**Figure 3:** A visualization of the regions with high mutual information, which make up 0.35% of the total space.

From Figure 3, we see that that peaks of non-trivial mutual information are sparse in the space of  $x_i, x_j$  pairs and have some structure. In particular, segments of non-trivial mutual information with slope 1 indicate portions of challenges that yield information about other challenges, which are apparently related. An adversary can use knowledge of this structure to more effectively guess response bits, thereby reducing the available entropy. In particular, the entropy is reduced to [Mae16]

$$H_{joint} = H_{min} - \sum_{i=0}^{n-1} I(x_i, x_{i+1}), \quad (9)$$

where the ordering of the bits is such that the penalty is as large as possible. Calculating the ordering of the bits to maximize the joint information penalty is effectively a traveling salesman problem, which we solve approximately with a 2-opt algorithm [CKT99]. The resulting entropy estimates are tabulated in Table 3, along with entropy density estimates defined analogously to Equation 7. Our estimates of the joint-entropy density is, on average, 5% less than our estimates of the min-entropy. This is similar to other electronic PUF designs, where the joint-entropy estimate is between 2.9% and 8.24% less. See Reference [Mae16] for a detailed comparison.

Although the existence of non-zero mutual information lowers the amount of information that can be securely exchanged, calculating the mutual information directly is a computationally inefficient task. Such estimates, and therefore such attacks, are difficult

**Table 3:** Min entropy, joint entropy, and joint entropy densities for  $N = 3 - 8$ . Joint entropy density estimates are similar to many other FPGA-based PUF designs.

$N$	$H_{min}$	$H_{joint}$	$\rho_{joint}$
3	14.5	14.4	0.80
4	39.1	37.9	0.79
5	117	110	0.73
6	301	285	0.79
7	725	661	0.75
8	1610	1340	0.66

to calculate for large  $N$ . Three-bit correlations almost certainly exist, but are even more difficult to estimate, so it's unclear that that entropy is much smaller than our joint-entropy estimates in practice, although a machine-learning attack may reveal such dependencies efficiently [RSS<sup>+</sup>10].

### 5.3 Context Tree Weighting Test

In this subsection, we estimate the entropy through a string compression test. In particular, we consider the context tree weighting (CTW) algorithm [WST95]. This algorithm takes a binary string called the *context* and forms an ensemble of models that predict subsequent bits in the string. It then losslessly compresses subsequent strings into a codeword using the prediction model. If the context contains information about a subsequent string, then the codeword will be of reduced size.

In the context of PUFs, the codeword length has been shown to approach the true entropy of the generating source in the limit of unbounded tree depth [ISS<sup>+</sup>06]. However, the required memory scales exponentially with tree depth, so it is not computationally feasible to consider an arbitrarily deep tree in the CTW algorithm. Instead, we vary the tree depth up to  $D = 20$  to optimize the compression. Nonetheless, the results in this section should be understood as an upper-bound for the true entropy, especially for larger  $N$ .

We perform a CTW compression as follows.

1. We collect data for  $N = 3 - 8$  HBN-PUFs with  $N_{oscs} = 32$ ,  $N_{chal} = N_{vc}$ , and  $N_{meas} = 1$ .
2. We concatenate the resulting measurements for all but one PUF instances into a 1D string of length  $(N_{oscs} - 1)N_{vc}N$  to be used as context.
3. We apply the CTW algorithm to compress the measurements from the last PUF with the context, using various tree depths to optimize the result.
4. We repeat steps 2-3, omitting measurements from a different PUF instance, until all PUFs have been compressed.

The results of this compression test are presented in Table 4.

The final entropy estimate is the average codeword length from all of the compression tests described above. If the behavior of the  $N_{oscs} - 1$  PUF instance can be used to predict the behavior of the unseen instance, then the PUFs do not have full entropy. The codeword length is simply the number of additional bits required to encode the PUF instance's challenge-response behavior.

Consistent with the expectation that this is an upper-bound estimate, the entropies are all larger than those calculated with the joint-entropy test in Section 5.2. Most of the PUF data is resistance to compression, particularly those with higher  $N$ , although

**Table 4:** Entropy and entropy density, as estimated from the CTW compression test. The entropy estimate is simply the average codeword length. Note that this is an upper-bound of the true entropy due to the bounded tree-depth.

$N$	$H_{CTW}$	$\rho_{CTW}$
3	17.9	0.993
4	43.8	0.913
5	148	0.984
6	356	0.99
7	882	1.00
8	2016	1.00

it is likely the case that higher  $N$  require a deeper tree to compress. These results are again similar to studies on other FPGA-based PUFs, which find CTW compression rates between 49% and 100% [KKR<sup>+</sup>12]. This test is another indication that HBN-PUFs have near full entropy.

## 5.4 Entropy Summary

In this section, we describe three different statistical tests to estimate the entropy in the HBN-PUFs. Two of the tests are computationally intensive and only performed on HBN-PUFs of size  $N = 3 - 8$ . One is more easily scalable, which we evaluate for  $N$  up to 64, but may be an overly optimistic estimate. To better understand these estimates as a function of  $N$  and resource size, these three estimates are shown in Figure 4.

The  $H_{CTW}$  estimate yields the most entropy, followed by  $H_{min}$  and  $H_{joint}$ . This is expected because  $H_{CTW}$  is an upper-bound estimate, while  $H_{joint}$  is equal to  $H_{min}$  with a penalty term determined by mutual information. Nonetheless, all three estimates are reasonably close, particularly on the scale in Figure 4. Further, the functional form of  $H_{min}$  is convex on a log-log scale, suggesting exponential growth with  $N$ .

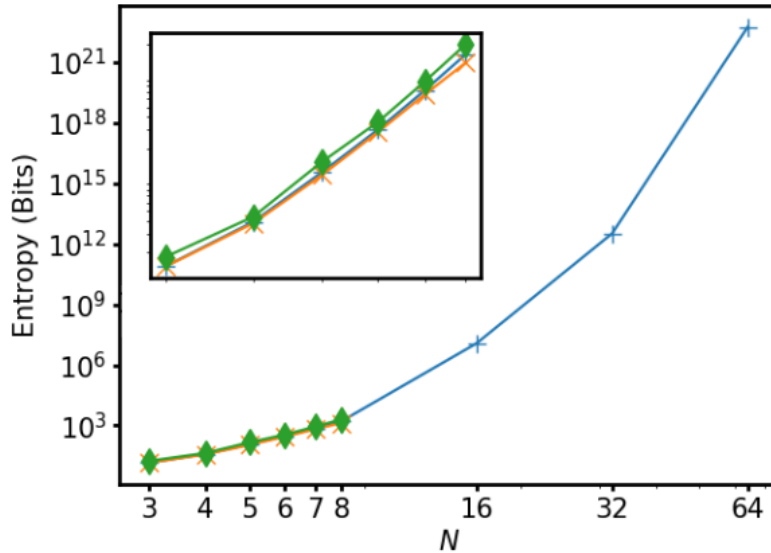


**Figure 4:** A summary of the entropy results. The  $H_{min}$  (blue) curve suggests exponential growth. All three curves are reasonably close within the  $N = 3 - 8$  window.

These results suggest that HBN-PUFs are not only strong in the sense that their challenge space is exponentially large in resource size, but that their entropy is exponentially large as well. This is important distinction because, for most security applications, a challenge-response pair that is knowable by an adversary is of no use. Many previously reported strong PUFs have been shown explicitly to be susceptible to model-building attacks [RSS<sup>+</sup>10]. Though it remains to be seen if the HBN-PUF is resistant to such attacks, the exponential scaling of the entropy estimates suggests this may not be the case.

## 6 Conclusions and Further Work

In this work, we introduce the concept of an HBN-PUF. We describe its construction on FPGAs and how the challenge-response process is executed. We quantify the uniqueness and reliability of HBN-PUF instances of varying size with standard intra- and inter-device statistics. Finally, we present three entropy estimates for HBN-PUF instances of varying size.

We find intra- and inter-device statistics in line with many previously reported PUF designs. They are close to ideal and have tight distributions, suggesting the HBN-PUFs to be candidates for device authentication purposes. Further, entropy estimates suggests HBN-PUFs are strong in the sense that their entropy scales exponentially with resource count. This means HBN-PUFs constructed from on the order of hundreds of LEs can efficiently store trillions or more independent cryptographic keys in their physical structure.

Several future lines of inquiry are suggested by this work. In particular, the impact of temperature and voltage variations is not studied here. Quantifying the response variation to varying environments is important for practical PUF applications [MSA<sup>+</sup>14] and deserves to be studied in the case of HBN-PUFs. Additionally, we have not studied the ability of machine learning techniques to perform a model-building attack. These attacks have been shown to make other strong PUFs vulnerable, and the question needs to be investigated here as well.

## 7 Acknowledgements

This material is based upon work supported by the Army STTR Program Office under Contract No. W31P4Q-19-C-0014.

## References

- [BH15] Rajdeep Bhanot and Rahul Hans. A review and comparative analysis of various encryption algorithms. *International Journal of Security and Its Applications*, 9(4):289–306, 2015.
- [CKT99] Barun Chandra, Howard Karloff, and Craig Tovey. New results on the old k-opt algorithm for the traveling salesman problem. *SIAM Journal on Computing*, 28(6):1998–2029, 1999.
- [DLHG16] Otti D’Huys, Johannes Lohmann, Nicholas D Haynes, and Daniel J Gauthier. Super-transient scaling in time-delay autonomous boolean network motifs. *Chaos: An Interdisciplinary Journal of Nonlinear Science*, 26(9):094810, 2016.
- [HBF09] Daniel E Holcomb, Wayne P Burleson, and Kevin Fu. Power-up sram state as an identifying fingerprint and source of true random numbers. *IEEE Transactions on Computers*, 58(9):1198–1210, 2009.

- [ISS<sup>+</sup>06] Tanya Ignatenko, Geert-Jan Schrijen, Boris Skoric, Pim Tuyls, and Frans Willems. Estimating the secrecy-rate of physical unclonable functions with the context-tree weighting method. In *2006 IEEE International Symposium on Information Theory*, pages 499–503. IEEE, 2006.
- [JK03] Jakob Jonsson and Burt Kaliski. Public-key cryptography standards (PKCS)# 1: RSA cryptography specifications version 2.1. Technical report, 2003.
- [KKR<sup>+</sup>12] Stefan Katzenbeisser, Ünal Kocabaş, Vladimir Rožić, Ahmad-Reza Sadeghi, Ingrid Verbauwhede, and Christian Wachsmann. PUFs: Myth, fact or busted? a security evaluation of physically unclonable functions (PUFs) cast in silicon. In *International Workshop on Cryptographic Hardware and Embedded Systems*, pages 283–301. Springer, 2012.
- [LHH18] Lin Liu, Hui Huang, and Shiyang Hu. Lorenz chaotic system-based carbon nanotube physical unclonable functions. *IEEE Transactions on Computer-Aided Design of Integrated Circuits and Systems*, 37(7):1408–1421, 2018.
- [Mae16] Roel Maes. *Physically unclonable functions*. Springer, 2016.
- [MBW<sup>+</sup>19] Thomas McGrath, Ibrahim E Bagci, Zhiming M Wang, Utz Roedig, and Robert J Young. A PUF taxonomy. *Applied Physics Reviews*, 6(1):011303, 2019.
- [MSA<sup>+</sup>14] Sanu K Mathew, Sudhir K Satpathy, Mark A Anders, Himanshu Kaul, Steven K Hsu, Amit Agarwal, Gregory K Chen, Rachael J Parker, Ram K Krishnamurthy, and Vivek De. 16.2 a 0.19 pj/b pvt-variation-tolerant hybrid physically unclonable function circuit for 100% stable secure key generation in 22 nm CMOS. In *2014 IEEE International Solid-State Circuits Conference Digest of Technical Papers (ISSCC)*, pages 278–279. IEEE, 2014.
- [RBK10] Ulrich Rührmair, Heike Busch, and Stefan Katzenbeisser. Strong pufs: models, constructions, and security proofs. In *Towards hardware-intrinsic security*, pages 79–96. Springer, 2010.
- [Ros15] David P Rosin. Ultra-fast physical generation of random numbers using hybrid boolean networks. In *Dynamics of Complex Autonomous Boolean Networks*, pages 57–79. Springer, 2015.
- [RRG13] David P Rosin, Damien Rontani, and Daniel J Gauthier. Ultrafast physical generation of random numbers using hybrid boolean networks. *Physical Review E*, 87(4):040902, 2013.
- [RSS<sup>+</sup>10] Ulrich Rührmair, Frank Sehnke, Jan Sölter, Gideon Dror, Srinivas Devadas, and Jürgen Schmidhuber. Modeling attacks on physical unclonable functions. In *Proceedings of the 17th ACM conference on Computer and communications security*, pages 237–249. ACM, 2010.
- [SvdSvdL12] Peter Simons, Erik van der Sluis, and Vincent van der Leest. Buskeeper PUFs, a promising alternative to d flip-flop PUFs. In *2012 IEEE International Symposium on Hardware-Oriented Security and Trust*, pages 7–12. IEEE, 2012.
- [TŠK07] Pim Tuyls, Boris Škoric, and Tom Kevenaar. *Security with noisy data: on private biometrics, secure key storage and anti-counterfeiting*. Springer Science & Business Media, 2007.

- [TŠS<sup>+</sup>05] Pim Tuyls, Boris Škorić, Sjoerd Stallinga, Anton HM Akkermans, and Wil Ophey. Information-theoretic security analysis of physical uncloneable functions. In *International Conference on Financial Cryptography and Data Security*, pages 141–155. Springer, 2005.
- [WST95] Frans MJ Willems, Yuri M Shtarkov, and Tjalling J Tjalkens. The context-tree weighting method: basic properties. *IEEE Transactions on Information Theory*, 41(3):653–664, 1995.
- [ZDMW16] Junqing Zhang, Trung Q Duong, Alan Marshall, and Roger Woods. Key generation from wireless channels: A review. *IEEE Access*, 4:614–626, 2016.

## A Verilog codes

In these appendices, we briefly present Verilog codes for synthesizing an HBN-PUF.

### A.1 Node

We present Verilog code for synthesizing a single HBN-PUF node in Listing 1. This node corresponds to the schematic in Figure 1f.

```

1 module Node(reset, challenge, inleft, inright, out);
2
3     input reset;
4     input challenge;
5     input inleft;
6     input inright;
7     output out;
8
9     wire node_internal;
10    wire node_external;
11
12    assign node_internal = inleft ^ node_external ^ inright;
13    assign node_external = reset ? challenge : node_internal;
14    assign out = node_external;
15
16 endmodule

```

### A.2 HBN-PUF

We present Verilog code for synthesizing a single HBN-PUF in Listing 2. This includes both the ABN described within the generate block (see also, Listing 1), and the synchronous components within the always block. For  $N = 16$ , the module corresponds to the HBN-PUF in Figure 1e.

```

1 module HBN_PUF(clk, reset, challenge, response);
2
3     parameter N = 2;
4
5     input clk;
6     input reset;
7     input [N-1:0] challenge;
8     output reg [N-1:0] response;
9
10    wire [N-1:0] ring_state /*synthesis keep*/;
11
12    genvar i;
13    generate
14    for (i=0; i<N; i=i+1) begin : generate_ring
15        Node n (

```

```
16         .reset(reset),
17         .challenge(challenge[i]),
18         .inleft(ring_state[(i+N-1)%N]),
19         .inright(ring_state[(i+1)%N]),
20         .out(ring_state[i])
21     );
22 end
23 endgenerate
24
25 always @(posedge clk) begin
26     response <= ring_state;
27 end
28
29 endmodule
```